SUPPLEMENTAL DATA

Study design and participants

Patients underwent imaging with ^{68}Ga-FAPI PET between October 2018 and October 2021 at the Department of Nuclear Medicine at the University Hospital Essen. This is an interim analysis of the ongoing ^{68}Ga-FAPI PET observational trial conducted at the University Hospital Essen (NCT04571086). Until October 2021, adult patients who underwent clinical ^{68}Ga-FAPI PET were offered the possibility to consent to a prospective observational trial for correlation and clinical follow-up of PET findings. Evaluation of data was approved by the ethics committee of the University Duisburg-Essen (20-9485-BO and 19-8991-BO). Patient subgroups have been reported in previous publications (N=47 (*1*), N=69 (*2*), N=91 (*3*)).

Anonymized study data were managed using the Research Electronic Data Capture (REDCap) electronic data capture tools hosted at the University Hospital Essen (*4,5*). TNM staging by ^{68}Ga-FAPI PET and ^{18}F-FDG PET was determined in accordance with American Joint Committee on Cancer (AJCC) criteria, 8th edition (*6*).

PET imaging and administration of radioligand

All patients gave written informed consent to undergo a clinical ^{68}Ga-FAPI PET scan. Initially, between the period of October 2018-2019, patients received ^{68}Ga-labeled FAPI-04 ligand (N=21), and from then on, FAPI-46 has been used in our clinic and thus was received by the majority of patients in this study (N=303). Radiosynthesis and labeling were performed as described previously (*7,8*). Median injected activity of ^{68}Ga-

FAPI was 112 MBq (interquartile range (IQR): 59). PET/CT datasets for ^{68}Ga-FAPI were acquired at a median of 14 minutes after injection based on previous assessment (*2*).

^{18}F-FDG PET scans were performed as per standard of care for oncologic indications. Patients were instructed to fast for at least 6 hours before the scan to achieve serum glucose levels of <150 mg/dl prior to the scan. Median injected activity of ^{18}F-FDG was 283 MBq (IQR: 182). PET/CT datasets for ^{18}F-FDG were acquired at a median of 67 minutes after injection.

Whole body images encompassing the patients' head to mid thighs were obtained. Images were acquired using Siemens 128mCT in 52/324 cases (16%), Siemens mCT VISION in 265/324 (82%), and Siemens mMR in 7/324 (2%). All devices are cross-calibrated based on EARL accreditation standards. All PET scans were acquired in 3D mode with an acquisition time of 3 to 5 min/bed position at all sites. The median time interval between ^{18}F-FDG and ^{68}Ga-FAPI PET was 0 days (IQR: 2). For patients who underwent both ^{18}F-FDG and ^{68}Ga-FAPI PET imaging (N=237), 159/237 (67%) had received both scans on the same day (with at least 4 hours between both scans).

Imaging analysis

Each scan was analyzed on five separate levels: Primary/regional tumor, regional lymph nodes, distant lymph nodes, visceral metastases and bone metastases. Spherical volumes of interest (VOI) were used to determine maximum standardized uptake values (SUV_{max}) as well as tumor volumes of the hottest lesion at every region. A 40% isocontouring approach was used to assess metabolic tumor volume. Tracer uptake in

normal organs was quantified by SUV_{mean} using 2-cm-diameter VOIs drawn at the center of each of the aortic arch, right liver lobe, and left gluteal muscle.

Tumor-to-background ratios (TBR) were determined to quantify the image contrast. TBR_{max} was calculated by dividing the maximum SUV of the tumor by the mean SUV of the respective background (blood, liver and muscle).

Immunohistochemistry and FAP Scoring

Paraffin blocks of histopathological samples (from surgery or biopsy) dated within 3 months from the date of ^{68}Ga-FAPI PET were retrieved, such that there was no change in treatment between sampling and PET. Adequate samples were prepared and stained with FAPα antibody as described by Kessler *et al*. (*1*). Overall percentage tumor and stroma were visually quantified for every sample, and a semi-quantitative analysis for tumor and stromal FAP staining was assessed by an experienced pathologist and graded as 0 (absence or weak FAPα immunostaining in <1% of cells), 1 (focal positivity in 1-10% of cells), 2 (11-50% of cells), and 3 (51-100% staining) for tumor and stroma staining separately, as reported previously by Henry *et al*. (*9*). In addition, an overall FAP score was included for each sample using the highest score assigned for tumor and stroma scores.

Statistical analysis

Descriptive statistics were calculated. For description of SUV, arithmetic mean and standard deviation were used. After testing the data for Gaussian distribution using the Shapiro-Wilk test, comparisons of SUV and TBR between ^{68}Ga-FAPI and ^{18}F-FDG across

tumor entities were carried out with a two-tailed paired t-test. Pearson correlation coefficient was used to assess the correlation between FAPα score and the SUV_{max}, and the correlation was interpreted as negligible ($0.00 < r \leq \pm 0.29$), low ($\pm 0.30 \leq r \leq \pm 0.49$), moderate ($\pm 0.50 \leq r \leq \pm 0.69$), or high ($r \geq \pm 0.70$) (*10*). A *p*-value of <0.05 was considered statistically significant. All statistical analyses were performed using SPSS Statistics Version 28 (IBM, Armonk, NY, USA) and Excel for Mac Version 15.25 (Microsoft, Redmond, Washington, USA). GraphPad Prism for Mac version 9.3.1 (GraphPad Software, San Diego, California, USA) was used for graphical visualization.

SUPPLEMENTAL FIGURES

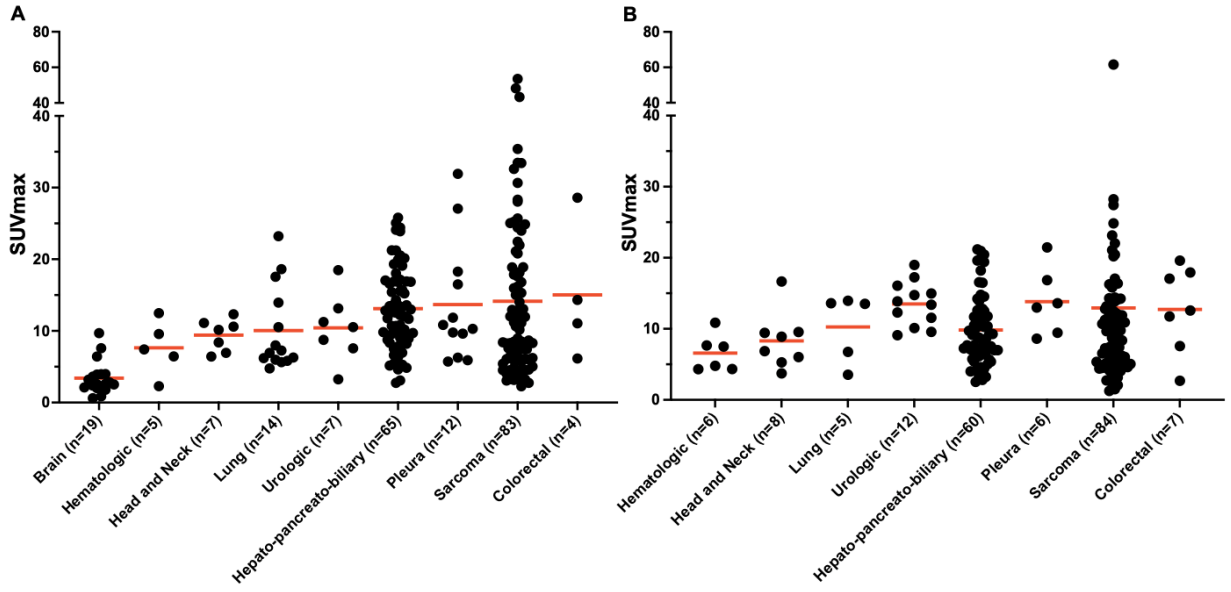

Supplemental figure 1. Mean SUV_{max} on ^{68}Ga-FAPI PET for **(A)** primary lesions (N=216) and **(B)** hottest metastatic lesions per patient (N=188) for larger subgroups (data points represent hottest lesions for individual patients). Numbers of patients included for every tumor entity are given on the x-axis. Red lines represent mean values. Y-axis is split to account for extreme values.

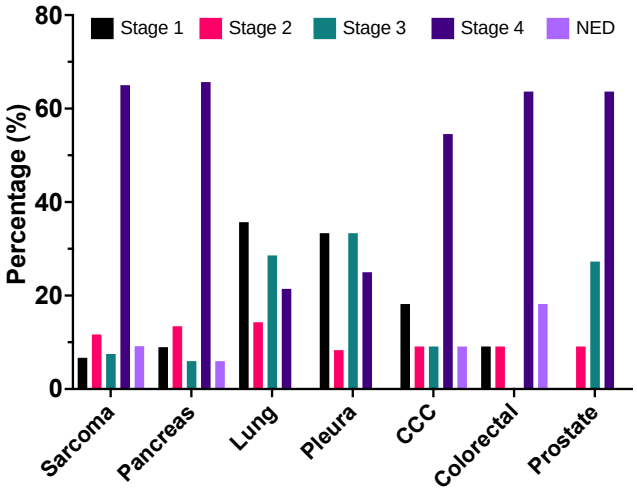

Supplemental figure 2. Staging with ^{68}Ga-FAPI PET across the seven most common tumor entities (except brain tumors and N=9 patients with sarcoma not stageable according to AJCC-8). N=248 total patients shown. M1 disease detected in majority of patients with tumors of the pancreas (44/67, 66%), sarcoma (79/122, 65%), tumors of the colon/rectum (7/11, 64%), prostate (7/11, 64%) and CCC (6/11, 55%). M0 disease detected mostly in tumors of the lung (11/14, 79%) and pleura (9/12, 75%).
CCC: cholangiocellular carcinoma; NED: no evidence of disease on ^{68}Ga-FAPI PET.

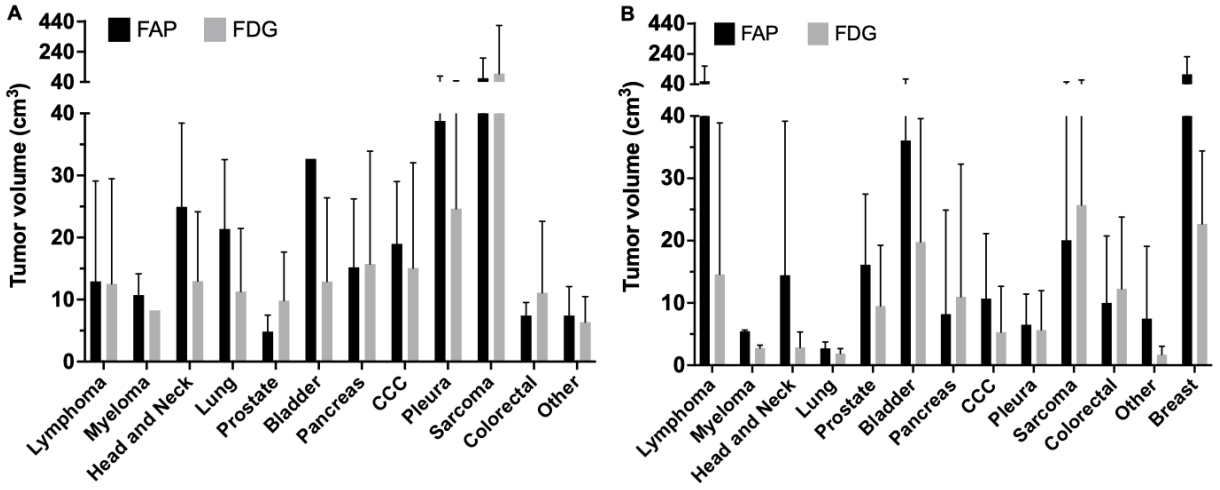

Supplemental figure 3. Comparison of tumor volumes for **(A)** primary lesions and **(B)** metastatic lesions between ^{68}Ga-FAPI and ^{18}F-FDG PET across all tumor entities. Mean and standard deviation are presented. Y-axis is split to account for extreme values.

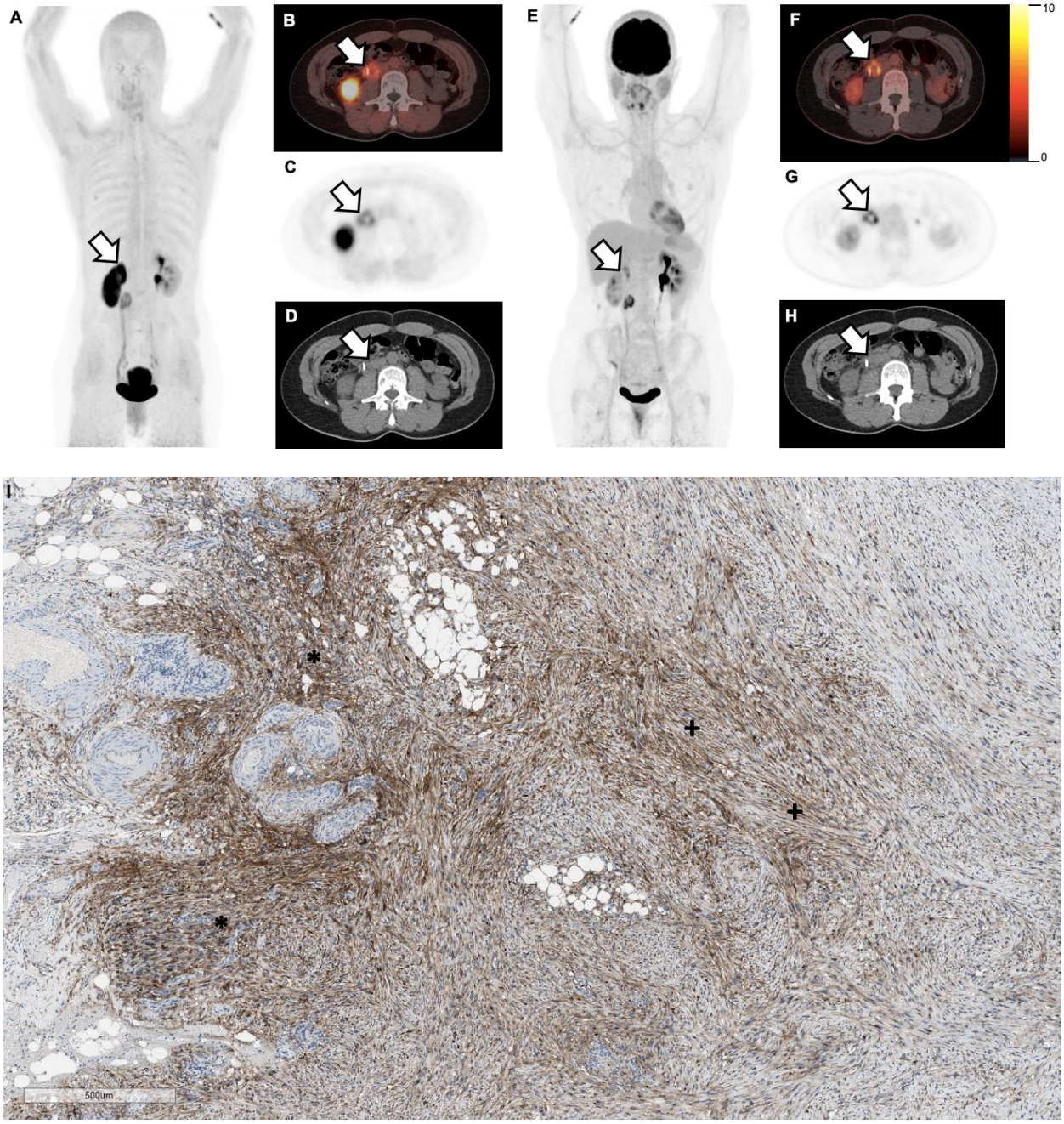

Supplemental figure 4 for a 52-year-old female with stage 2 spindle cell sarcoma (T2N0M0, G3). (A) FAPI maximum-intensity projection **(B)** fused FAPI PET/CT **(C)** FAPI PET and **(D)** accompanying low dose CT along with concomitant **(E)** FDG maximum-intensity projection **(F)** fused FDG PET/CT **(G)** FDG PET and **(H)** accompanying high dose CT. Arrows point towards visceral metastases in the right peritoneum (FAP SUVmax 6.1, FDG SUVmax 10.8). **(I)** Immunohistochemical staining with FAP antibody of a sample from the specific region reveals areas of tumor staining (>50%, score 3+; asterisks) and stromal staining (>50%, score 3+; plus sign). Overall FAP score: 3.

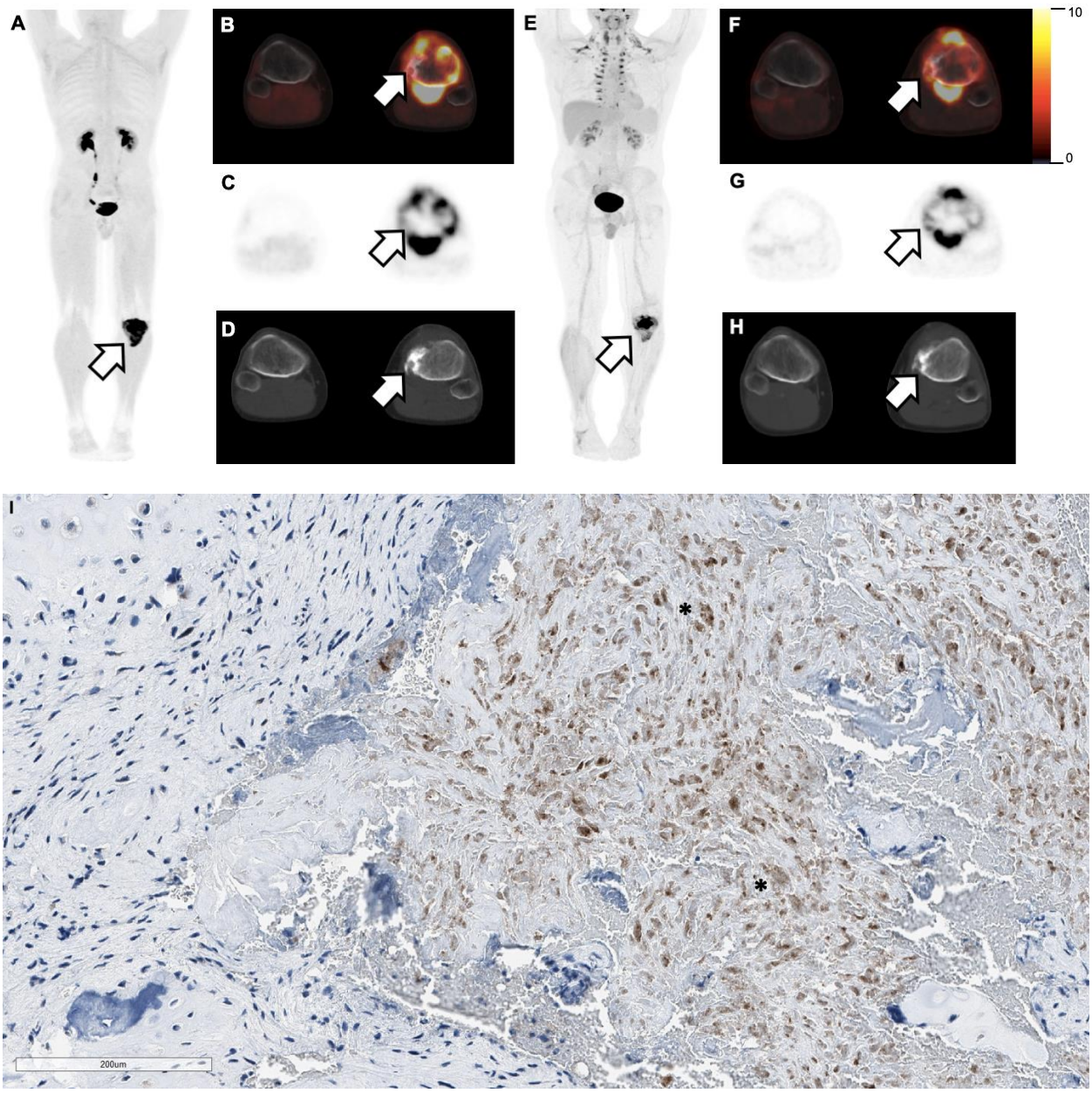

Supplemental figure 5 for a 19-year-old male with stage 2B osteosarcoma (T2N0M0, G3). **(A)** FAPI maximum-intensity projection **(B)** fused FAPI PET/CT **(C)** FAPI PET and **(D)** accompanying low dose CT along with concomitant **(E)** FDG maximum-intensity projection **(F)** fused FDG PET/CT **(G)** FDG PET and **(H)** accompanying high dose CT. Arrows point towards primary lesion in the proximal left tibia (FAP SUVmax 24.4, FDG SUVmax 18.2). **(I)** Immunohistochemical staining with FAP antibody of a sample from the specific region reveals areas of tumor staining (>50%, score 3+, asterisks). Overall FAP score: 3.

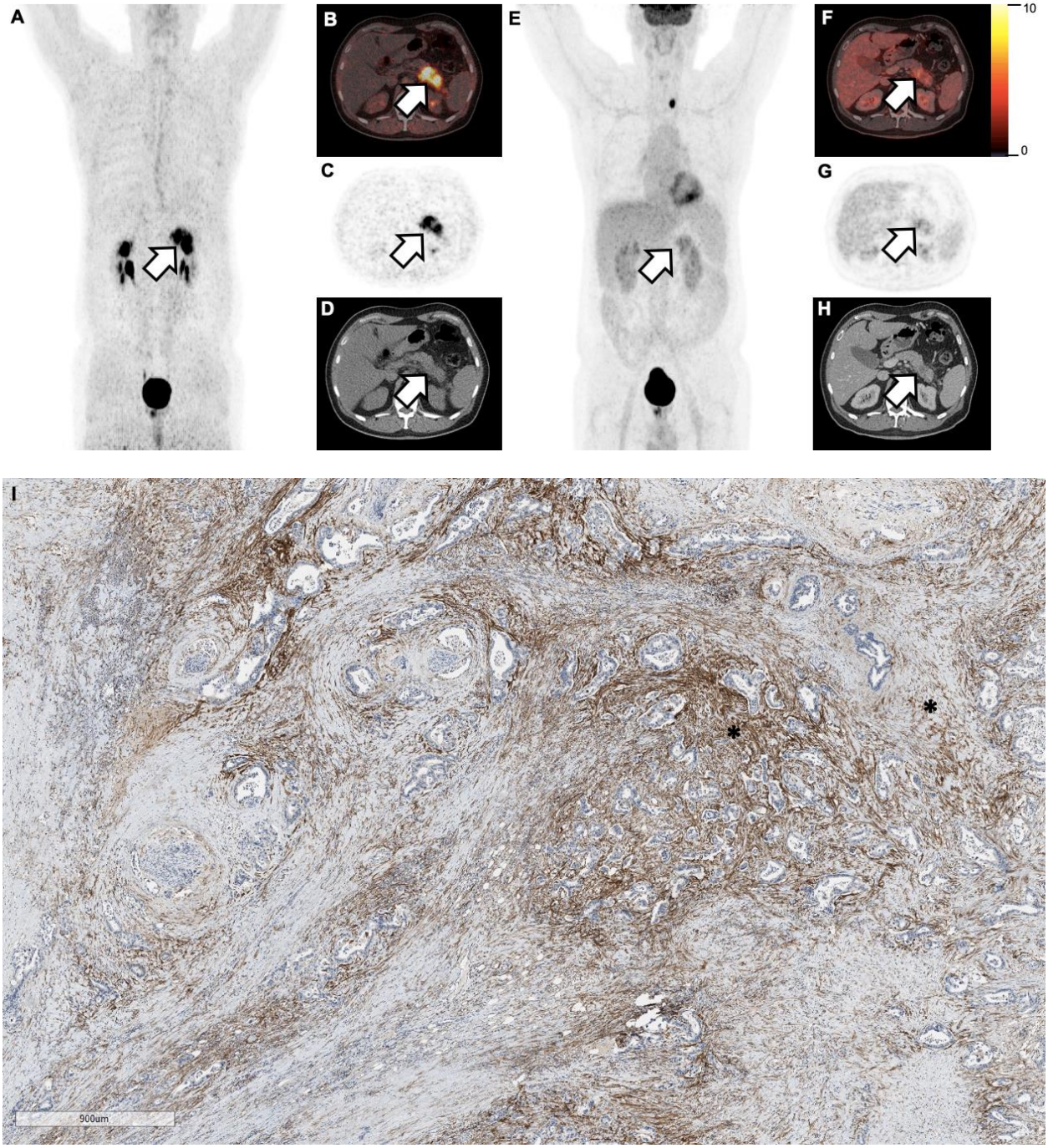

Supplemental figure 6 for a 57-year-old male with stage 1B pancreatic adenocarcinoma (T2N0M0). (A) FAPI maximum-intensity projection **(B)** fused FAPI PET/CT **(C)** FAPI PET and **(D)** accompanying low dose CT along with concomitant **(E)** FDG maximum-intensity projection **(F)** fused FDG PET/CT **(G)** FDG PET and **(H)** accompanying high dose CT. Arrows point towards primary lesion in the pancreas (FAP SUVmax 25.1, FDG SUVmax 6.2). **(I)** Immunohistochemical staining with FAP antibody of a sample from the specific region reveals areas of stromal staining (>50%, score 3+, asterisks). Overall FAP score: 3.

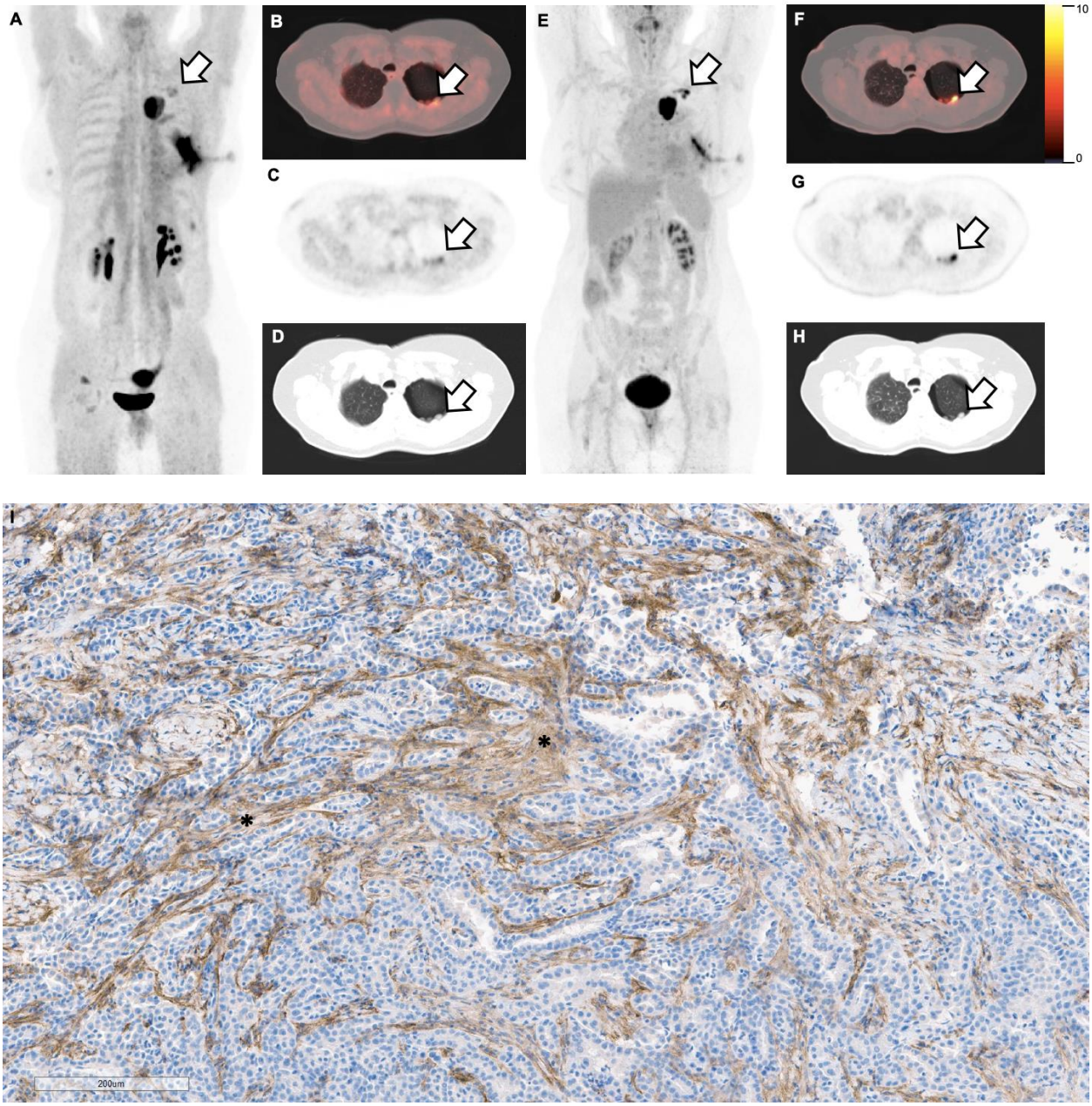

Supplemental figure 7 for a 66-year-old female with stage 2 pleural mesothelioma (T1/2N1M0). (A) FAPI maximum-intensity projection **(B)** fused FAPI PET/CT **(C)** FAPI PET and **(D)** accompanying low dose CT along with concomitant **(E)** FDG maximum-intensity projection **(F)** fused FDG PET/CT **(G)** FDG PET and **(H)** accompanying high dose CT. Arrows point towards one of the primary lesions in the left parietal dorso-apical pleura (FAP SUVmax 5.9, FDG SUVmax 11.1). **(I)** Immunohistochemical staining with FAP antibody of a sample from the specific region reveals areas of stromal staining (>50%, score 3+). Overall FAP score: 3.

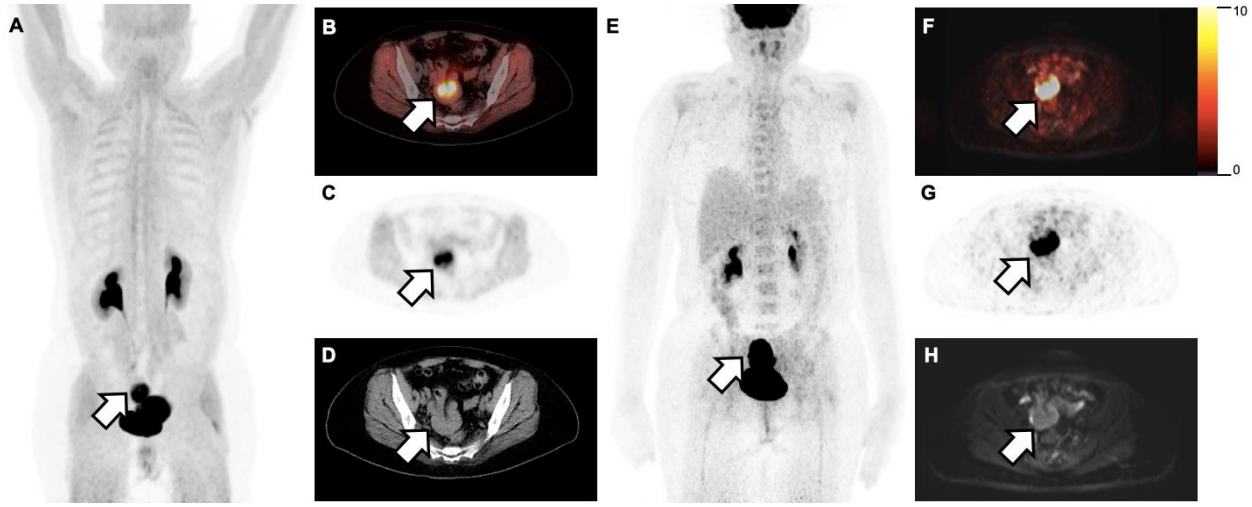

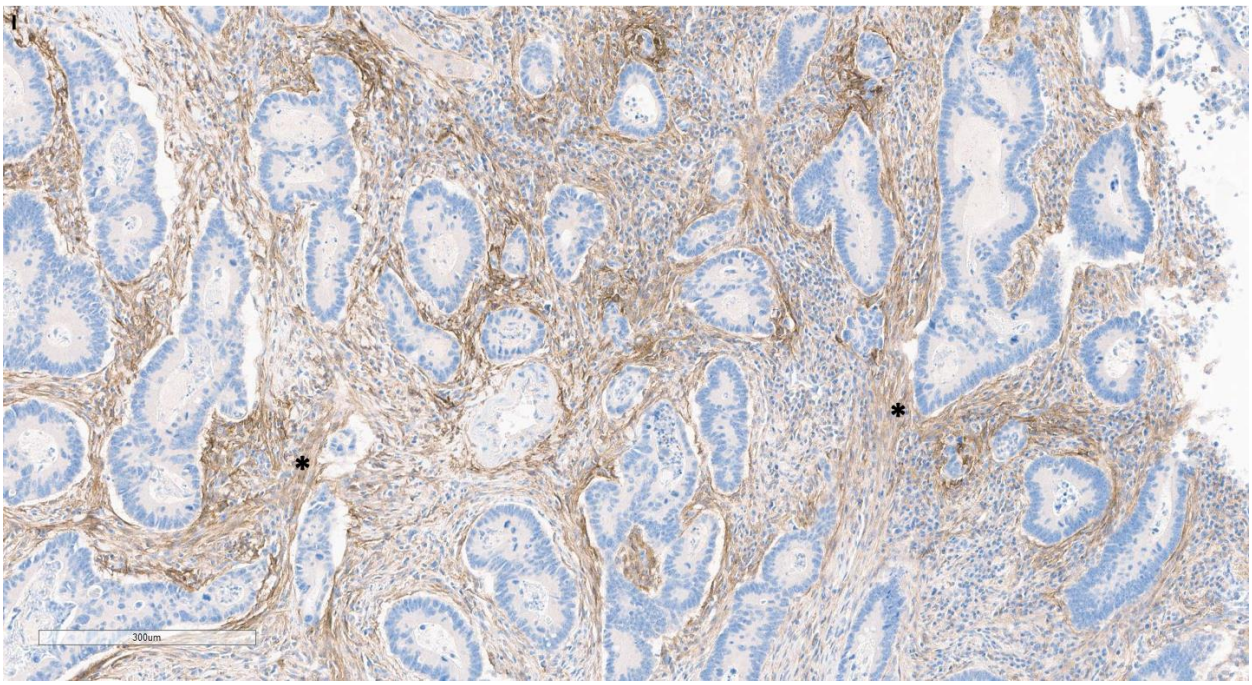

Supplemental figure 8 for a 55-year-old female with stage 2A colon adenocarcinoma (T3N0M0). (A) FAPI maximum-intensity projection **(B)** fused FAPI PET/CT **(C)** FAPI PET and **(D)** accompanying low dose CT along with concomitant **(E)** FDG maximum-intensity projection **(F)** fused FDG PET/MRI **(G)** FDG PET and **(H)** accompanying MRI. Arrows point towards the primary lesion in the left colon (FAP SUVmax 14.3, FDG SUVmax 41.3). **(I)** Immunohistochemical staining with FAP antibody of a sample from the specific region reveals areas of stromal staining (>50%, score 3+, asterisks). Overall FAP score: 3.

SUPPLEMENTAL TABLES

Supplemental Table 1. Breakdown of histopathological diagnoses as well as primary and metastatic lesions across tumor entities (N=324)

Tumor entities	Total N (% of total)	Primary lesions only, N (% of entity)	Metastatic lesions only*, N (% of entity)	Concomitant primary and metastatic lesions, N (% of entity)	NED, N (% of entity)
Sarcomas	**131 (40)**				
Angiosarcoma	2 (1)				
Chondrosarcoma	10 (3)				
Chordoma	7 (2)				
Clear cell sarcoma	3 (1)				
Endometrial sarcoma	3 (1)				
Ewing sarcoma	5 (2)				
Fibrosarcoma	11 (3)				
Gastrointestinal stromal tumors	2 (1)				
Leiomyosarcoma	9 (3)	39 (30)	40 (31)	44 (33)	8 (6)
Liposarcoma	16 (5)				
Osteosarcoma	13 (4)				
Other[+]	11 (3)				
Pleomorphic sarcoma	9 (3)				
Rhabdomyosarcoma	3 (1)				
Round cell sarcoma	2 (1)				
Solitary fibrous tumor	13 (4)				
Spindle cell sarcoma	7 (2)				
Synovial sarcoma	5 (2)				
Pancreas	**67 (21)**				
Acinar cell carcinoma	1 (0)				
Ductal adenocarcinoma	62 (19)				
Intraductal papillary mucinous neoplasia	1 (0)	14 (21)	10 (15)	42 (63)	1 (1)
Neuroendocrine carcinoma	1 (0)				
Signet ring cell carcinoma	1 (0)				
Unknown	1 (0)				
Brain	**22 (7)**				
Astrocytoma	1 (0)	19 (86)	0	0	3 (14)
Glioblastoma multiforme	19 (6)				
Unknown	2 (1)				
Lung	**14 (4)**				
Adenocarcinoma	5 (2)	9 (64)	0	5 (36)	0
Adenosquamous carcinoma	6 (2)				
Squamous cell carcinoma	3 (1)				
Pleura	**12 (4)**				
Biphasic mesothelioma	1 (0)	6 (50)	0	6 (50)	0
Epithelial mesothelioma	10 (3)				

Sarcomatoid mesothelioma	1 (0)				
Cholangiocellular carcinoma (CCC)	**11 (3)**				
Extrahepatic CCC (Klatskin tumor)	2 (1)	2 (18)	2 (18)	6 (55)	1 (9)
Extrahepatic CCC (non-Klatskin tumor)	2 (1)				
Intrahepatic CCC	7 (2)				
Colorectal	**11 (3)**				
Colon adenocarcinoma	6 (2)	2 (18)	5 (46)	2 (18)	2 (18)
Rectal adenocarcinoma	5 (2)				
Prostate	**11 (3)**	4 (36)	5 (46)	2 (18)	0
Adenocarcinoma	11 (3)				
Head and Neck	**9 (3)**				
Adenoid cystic carcinoma	5 (2)				
Polymorphic adenocarcinoma	1 (0)	1 (11)	2 (22)	6 (67)	0
Small blue round cell tumor	1 (0)				
Squamous cell carcinoma	2 (1)				
Bladder	**8 (3)**	0	4 (50)	1 (12)	3 (38)
Urothelial carcinoma	8 (3)				
Lymphoma	**7 (2)**				
NHL, diffuse large B-cell lymphoma	1 (0)	1 (14)	3 (43)	1 (14)	2 (29)
NHL, follicular lymphoma	5 (2)				
MALT lymphoma	1 (0)				
Myeloma	**6 (2)**				
IgA kappa	2 (1)				
IgG kappa	2 (1)	1 (17)	0	2 (33)	3 (50)
Light chain kappa	1 (0)				
Smouldering myeloma	1 (0)				
Ovarian	**4 (1)**				
Other	1 (0)	0	1 (25)	2 (50)	1 (25)
Serous carcinoma	3 (1)				
Breast	**3 (1)**	0	3 (100)	0	0
Tripe negative adenocarcinoma	3 (1)				
Duodenum	**2 (1)**	0	1 (50)	0	1 (50)
Duodenal adenocarcinoma	2 (1)				
Other	**6 (2)**				
Cervix, squamous cell carcinoma	1 (0)				
Knee, myoepithelial carcinoma	1 (0)				
Liver, hepatocellular carcinoma	1 (0)	2 (33)	2 (33)	2 (33)	0
Skin, melanoma	1 (0)				
Stomach, gastric adenocarcinoma	1 (0)				
Thyroid, papillary carcinoma	1 (0)				

MALT: mucosal associated lymphoid tissue; NED: no evidence of disease; NHL: non-Hodgkin's lymphoma.
* Refers to loco-regional or distant metastasis.
+ Each entity (N=1): Epitheloid sarcoma, follicular dendritic sarcoma, giant cell tumor, gastrointestinal neuroendocrine tumor (G-NET), hemangioendothelioma, hemangiopericytoma, myofibroblastic sarcoma, peripheral nerve sheath tumor, soft tissue sarcoma, synchronous adenosarcoma-carcinoma, vulvar sarcoma.

Supplemental Table 2. Comparison of average SUV_{max} (hottest lesion) and total number of involved regions (sum among all N=237 patients in the head-to-head comparison) between ^{68}Ga-FAPI and ^{18}F-FDG PET. Data are listed separate for non-metastatic versus distant metastatic disease by different tumor entities

	Non-metastatic (M0)				Metastatic (M1)			
	SUVmax		N involved regions		SUVmax		N involved regions	
	FAPI	FDG	FAPI	FDG	FAPI	FDG	FAPI	FDG
Lymphoma (N=6)	-	-	-	-	10.1	19.7	7	10
Myeloma (N=4)	6.9	6.3	4	3	-	-	-	-
Head and neck (N=6)	-	-	-	-	9.6	10.5	15	13
Lung (N=5)	12.8	9.4	4	4	18.6	13.4	9	8
Prostate (N=11)	7.7	3.4	4	3	15.8	7.9	20	20
Bladder (N=7)	-	19.1	-	1	10.5	7.8	8	7
Pancreas (N=41)	13.1	4.8	21	20	12.2	7.0	65	57
CCC (N=10)	17.2	6.0	5	5	8.2	9.4	12	11
Pleura (N=9)	11.0	11.6	11	11	24.2	15.0	8	8
Sarcoma (N=116)	13.7	8.9	52	48	14.3	9.7	137	131
Colorectal (N=10)	12.7	23.1	2	2	17.4	15.9	9	9
Other (N=12)	9.1	7.1	5	5	7.9	17.2	17	17

CCC: cholangiocellular carcinoma.

SUPPLEMENTAL REFERENCES

1. Kessler L, Ferdinandus J, Hirmas N, et al. (68)Ga-FAPI as a diagnostic tool in sarcoma: Data from the (68)Ga-FAPI PET prospective observational trial. *J Nucl Med.* 2022;63:89-95.

2. Ferdinandus J, Kessler L, Hirmas N, et al. Equivalent tumor detection for early and late FAPI-46 PET acquisition. *Eur J Nucl Med Mol Imaging.* 2021;48:3221-3227.

3. Kessler L, Ferdinandus J, Hirmas N, et al. Pitfalls and common findings in (68)Ga-FAPI-PET - A pictorial analysis. *J Nucl Med.* 2022;63:890-896.

4. Harris PA, Taylor R, Minor BL, et al. The REDCap consortium: Building an international community of software platform partners. *J Biomed Inform.* 2019;95:103208.

5. Harris PA, Taylor R, Thielke R, Payne J, Gonzalez N, Conde JG. Research electronic data capture (REDCap)--a metadata-driven methodology and workflow process for providing translational research informatics support. *J Biomed Inform.* 2009;42:377-381.

6. Amin MB, Edge S, Greene F, et al. *AJCC Cancer Staging Manual.* 8th ed. Springer International Publishing; 2017:55-986.

7. Lindner T, Loktev A, Giesel F, Kratochwil C, Altmann A, Haberkorn U. Targeting of activated fibroblasts for imaging and therapy. *EJNMMI Radiopharm Chem.* 2019;4:16.

8. Loktev A, Lindner T, Burger EM, et al. Development of fibroblast activation protein-targeted radiotracers with Improved tumor retention. *J Nucl Med.* 2019;60:1421-1429.

9. Henry LR, Lee HO, Lee JS, et al. Clinical implications of fibroblast activation protein in patients with colon cancer. *Clin Cancer Res.* 2007;13:1736-1741.

10. Hinkle DE, Wiersma W, Jurs SG. *Applied Statistics for the Behavioral Sciences*. 2nd ed. Boston: Houghton Mifflin; 2003: 118.